JOURNAL OF AIRCRAFT
Vol. 40, No. 3, May–June 2003

Vibration Control of a Landing Gear System Featuring Electrorheological/Magnetorheological Fluids

Young-Tai Choi* and Norman M. Wereley†
University of Maryland, College Park, Maryland 20742

The feasibility and effectiveness of electrorheological (ER) and magnetorheological (MR) fluid-based landing gear systems on attenuating dynamic load and vibration due to the landing impact are demonstrated. First, the theoretical model for ER/MR shock struts, which are the main components of the landing gear system, is developed based on experimental data. The analysis of a telescopic-type landing gear system using the ER/MR shock struts is theoretically constructed, and its governing equation is derived. A sliding mode controller, designed to be robust against parameter variations and external disturbances, is formulated, and controlled performance of the simulated ER/MR landing gear system is theoretically evaluated during touchdown of the aircraft.

Introduction

DURING touchdown, an aircraft is exposed to a short-duration impulsive impact. The landing impact has been recognized as a significant factor in structural fatigue damage, dynamic stress on the aircraft airframe, and crew and passenger discomfort. To attenuate the landing impact transmitted to aircraft, several types of landing gear systems have been employed in commercial airplanes. One potential method in which to implement landing gear systems is to use smart fluids such as electrorheological (ER) and magnetorheological (MR) fluids. In general, ER and MR fluids are known to have the outstanding advantages of continuously controllable rheological properties and fast response time in response to applied electric (ER) or magnetic (MR) field.[1,2] Therefore, landing gear systems using ER or MR fluids have salient features such as continuously controllable mechanical damping characteristics and wide control bandwidth.

Thus far, of the research published, studies of the application of ER and MR fluids to landing gear systems are largely unexplored.[3–14] Consequently, the main contribution of this study is to demonstrate the feasibility and effectiveness of ER and MR fluid-based landing gear systems on attenuating dynamic load and vibration due to the landing impact. To achieve this goal, the theoretical model for ER/MR shock struts, which are the main components of the landing gear system, is developed based on experimental data obtained at different excitation velocities and fields. With the theoretical model, the landing gear system using ER/MR shock struts is theoretically constructed, and its governing equation is derived. From the obtained governing equation, a sliding mode controller, which is robust against parameter variations and external disturbances, is formulated to attenuate the acceleration and displacement of the landing gear system. Controlled performances of the simulated landing gear system using the robust sliding mode controller are theoretically evaluated during touchdown of the aircraft.

ER/MR Shock Struts

A schematic diagram of the flow-mode type of controllable ER/MR shock struts proposed in this study is shown in Fig. 1. The shock struts are composed of gas and hydraulic reservoirs. The hydraulic reservoir is divided into upper and lower chambers by the piston head and fully filled with controllable fluids. There is a valve through the piston head, typically an annular valve, where the fluid is activated through the application of the field. As the piston moves, the resulting pressure moves fluids through the annular gap from the upper chamber to lower chamber. To compensate for the changing fluid volume occupied by the piston rod in the lower chamber, a gas accumulator is located above the upper chamber. In the absence of an external field, the ER/MR shock struts produce the same level of damping force as passive shock struts comprised of viscous damping force, gas spring force, and so forth. However, when the field is applied to the controllable fluid shock strut, additional damping force due to the field-induced yield stress is produced in the annular valve. This damping force can be continuously controlled by adjusting the intensity of the applied field.

The force of the ER/MR shock strut, F_d, can be expressed as a combination of nonlinear viscous damping, F_v, gas spring, F_g, and yield F_y forces:

$$F_d = F_v + F_g + F_y \tag{1}$$

The nonlinear viscous damping force F_v can be given by

$$F_v = c(\dot{v}, G)\dot{v} \tag{2}$$

where $\dot{v}$ is the relative velocity of shock strut, or shaft speed relative to the damper body, and G is the applied field. In the case of ER fluids, $G(=E)$ is the electric field that is proportional to applied voltage. In the case of MR fluids, $G(=H)$ is the magnetic field that is proportional to applied current. The function $c(\dot{v}, G)$ is the nonlinear viscous damping as a function of the relative velocity and applied field. In the ideal Bingham model, the postyield viscous damping of the ER/MR damper is changed by neither velocity nor the applied field. However, this assumption is valid only for conditions of low velocity and low field strength.[8,14] Because shock struts would normally operate under the conditions of high velocity and high field strength, assumption of constant postyield viscous damping is not sufficient to predict the behavior of the strut precisely. Therefore, in this study, a variable damping $c(\dot{v}, G)$ is used to predict the behavior of the struts, and the values of $c(\dot{v}, G)$ are identified through experiments. To do so, first, the damping force of a shock strut is tested under different piston velocities and field strengths. Next, from the measured data, the viscous damping is estimated over each piston velocity and applied field through a curve-fitting method. Then, a lookup table for the viscous damping is made using piston velocity and the applied field as the independent variables. The viscous damping at the untested conditions between experimentally estimated data is obtained via a linear interpolation.

Received 28 December 2001; revision received 21 June 2002; accepted for publication 28 June 2002.

*Research Assistant, Alfred Gessow Rotorcraft Center, Department of Aerospace Engineering; nicechoi@eng.umd.edu.

†Associate Professor, Alfred Gessow Rotorcraft Center, Department of Aerospace Engineering; wereley@eng.umd.edu. Associate Fellow AIAA.

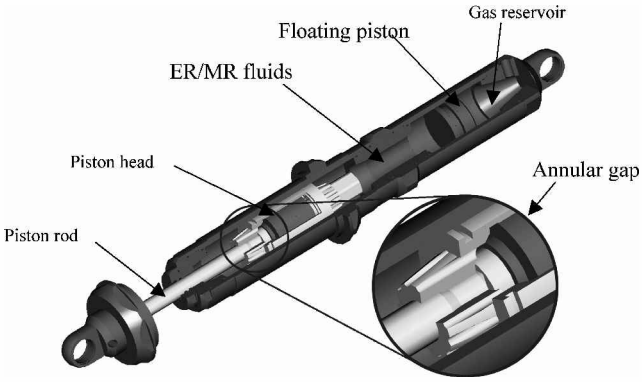

Fig. 1 Schematic diagram of the controllable ER/MR shock strut.

Because the gas in the pneumatic reservoir undergoes a polytropic process during touchdown, the gas spring force F_g due to the gas pressure can be given by[15]

$$F_g = A_r P_{g0}\left(\frac{V_{g0}}{V_{g0} - A_r v}\right)^n \tag{3}$$

where V_{g0} is the initial volume of the pneumatic chamber, P_{g0} is the initial gas pressure of the pneumatic chamber, and n is the polytropic exponent.

The yield force F_y due to the yield stresses of ER and MR fluids is given by[4]

$$F_y = (A_p - A_r)2(L/h)\tau_y(G)\,\mathrm{sgn}(\dot{v}) \tag{4}$$

where A_p is the cross-sectional area of piston head, A_r is the cross-sectional area of piston rod, L is the field activation length, h is the field activation gap, and $\tau_y(G)$ is the yield stress of the ER or MR fluid. It is well known that τ_y is an exponential function of applied field, $\tau_y = \alpha G^{\beta}$. Here, α and β are characteristic values determined by experiments.

To validate our theoretical model for the ER/MR shock struts, an ER shock strut was fabricated and tested. The requiring damping force level of the ER shock strut in this study is chosen on the basis of the conventional shock strut for a helicopter tail landing gear.[16] The electrode length L and gap h of the ER shock strut are 43 and 0.6 mm. For the ER fluid, laboratory-made ER fluid composed of 60% peanut oil and 40% corn starch particles by weight ratio was used, and its yield stress was experimentally obtained using a flow-mode device in which the fluid passes through an annular valve. The exponential function for the yield stress of the ER fluid was determined to be $\tau_y(E) = 193E^{1.3}$ Pa, and E is in kilovolts per millimeter. The fabricated ER shock strut and experimental setup for damping force testing is shown in Fig. 2. The fabricated ER shock strut is placed between the load cell and a hydraulic excitation actuator. The load cell is fixed, and the bottom part of the ER shock strut is moved through the hydraulic excitation actuator. When the piston of the ER shock strut moves along with the excitation actuator, the ER shock strut produces the damping force, and it is measured through the load cell.

Figure 3 shows the maximum damping force performance of the ER shock strut at different maximum piston velocities. In this case, each maximum piston velocity is obtained by increasing the excitation frequency of the sinusoidal function with a constant displacement amplitude of 15 mm. Note that the displacement amplitude of 15 mm was chosen to achieve high piston velocity on the basis of the capacity of the hydraulic excitation actuator. Below the maximum piston velocity of 0.2 m/s, it is clearly observed that the damping force increases as the applied electric field increases. However, over 0.2 m/s, the increment of the damping force in response to the applied field decreases. It arises from the fact that as the fluid velocity in the gap of the strut increases, the particle chains in the fluid are easier to break.[14] Figure 4 presents the viscous damping estimated by a curve-fitting method with the measured data. In Fig. 4, the solid

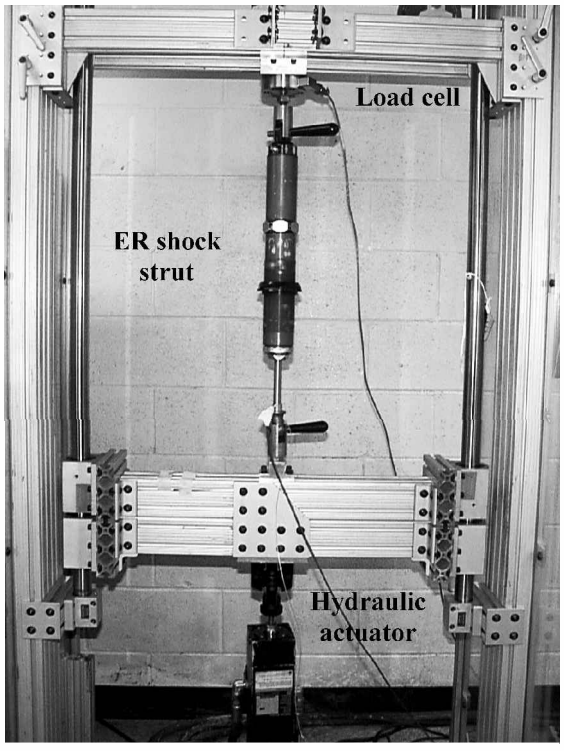

Fig. 2 Experimental setup for damping force testing of the ER/MR shock strut.

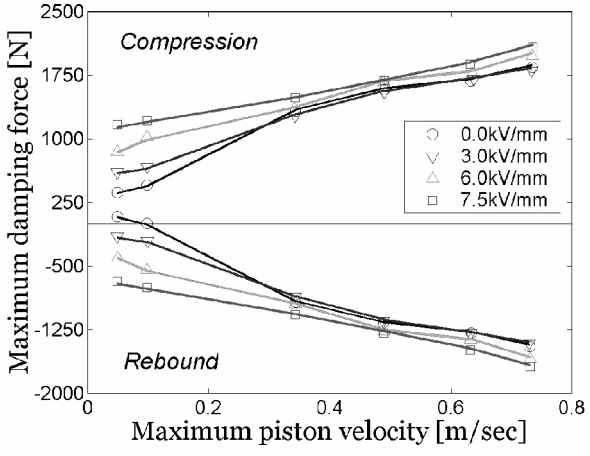

Fig. 3 Maximum damping force vs piston velocity.

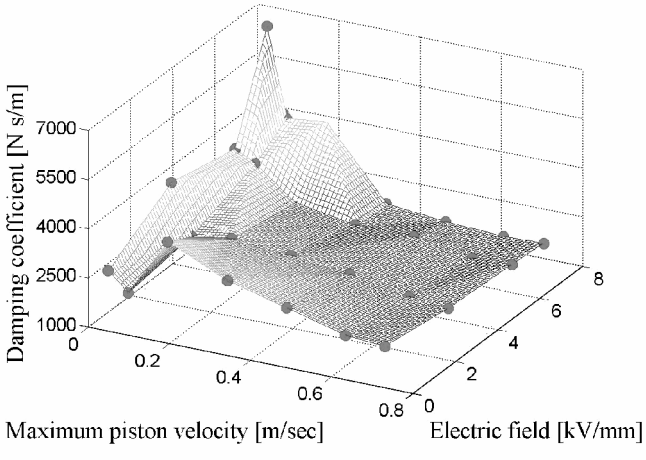

Fig. 4 Estimated damping coefficient.

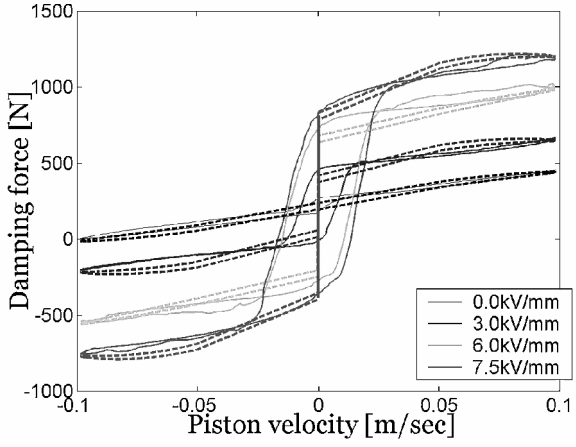

Damping force vs piston velocity

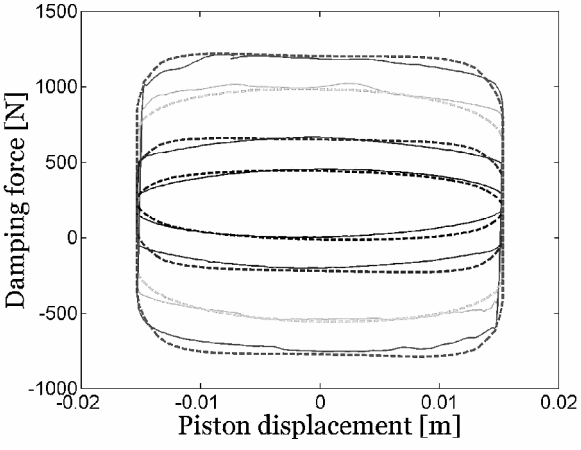

Damping force vs piston displacement

Fig. 5 Comparison between theoretical (– – –) and experimental (——) data (1.0 Hz and ±15 mm).

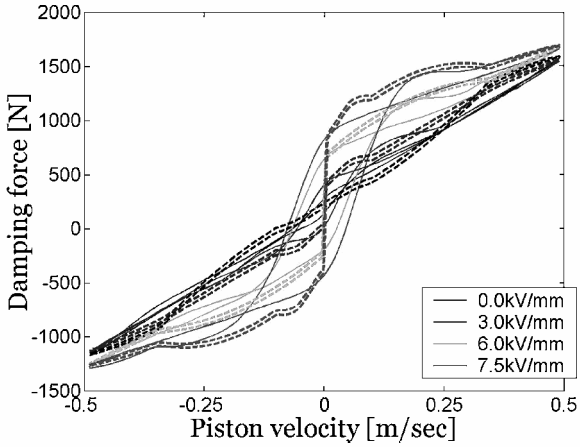

Damping force vs piston velocity

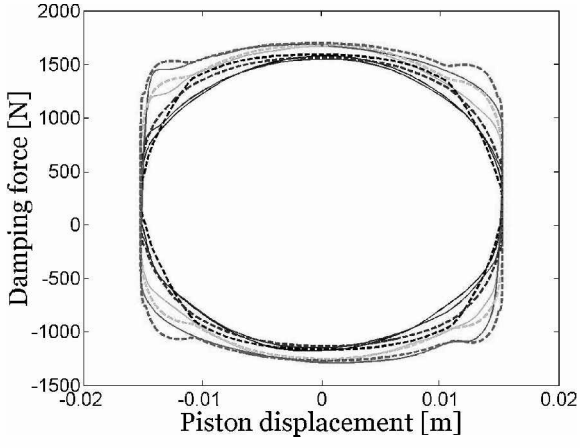

Damping force vs piston displacement

Fig. 6 Comparison between theoretical (– – –) and experimental (——) data (5.0 Hz and ±15 mm).

circle stands for the viscous damping directly estimated from the measured damping force characteristics. The viscous damping between the directly estimated values is obtained via an interpolation method.

Figure 5 presents a comparison between the theoretical and experimental data for the ER shock strut at the low maximum piston velocity condition of 0.094 m/s. In this case, the excitation frequency and amplitude are 1.0 Hz and 15 mm, respectively. As observed in Fig. 5, the theoretical data show favorable agreement with the experimental data. Note that the damping force of the ER shock strut is biased from zero because of the gas spring force from the gas accumulator. Figure 6 presents a comparison at the high maximum piston velocity condition of 0.471 m/s. In this case, the excitation frequency and amplitude are 5.0 Hz and 15 mm, respectively. As expected, the curve-fit model is still in a favorable accordance with the experimental data. Therefore, it is proved that the proposed theoretical model for the ER shock strut is appropriate for predicting its behavior with respect to the applied field.

Simulated ER/MR Landing Gear System

In general, there are several types of landing gear systems. Our analysis will focus on a telescopic type of landing gear system. The transient behavior of the landing gear system can be easily evaluated because the telescopic type of landing gear has no linkage mechanism. The schematic configuration of the landing gear system considered in this analysis is shown in Fig. 7. Note that our analysis is based on the assumption that the airframe is a rigid-body mass (the upper mass) and the wheel tire is a rigid-body mass (the lower mass) and nonlinear spring.

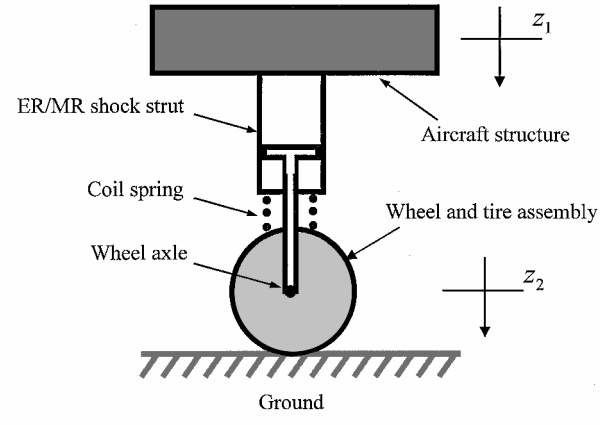

Fig. 7 Schematic configuration of telescopic type of ER/MR landing gear system.

The equations of motion for the landing gear system can be expressed as

$$(W_1/g)\ddot{z}_1 + F_{ds} + L_f - W_1 = 0$$
$$(W_2/g)\ddot{z}_2 - F_{ds} + F_t - W_2 = 0 \qquad (5)$$

where W_1 is the weight of the airframe, W_2 is the weight of the wheel tire, g is the gravitation acceleration, L_f is the lift force, z_1 is the displacement of the weight of the airframe, and z_2 is the displacement of the weight of the wheel tire. During the landing, the lift force varies and can be represented by[17]

$$L_f = [1.2 - 0.9\tanh(3t)](W_1 + W_2) \qquad (6)$$

where $t \geq 0$ is the time in seconds. F_{ds} is the damping force of the ER/MR shock strut with the coil spring given by

$$F_{ds} = F_d + F_s \tag{7}$$

The coil spring force is given by

$$F_s = k_s(z_1 - z_2) \tag{8}$$

where k_s is the stiffness coefficient of the coil spring. In addition, F_t is the wheel tire spring force and can be represented by

$$F_t = m\, z_2^r \tag{9}$$

where m and r are constants corresponding to various regimes of the tire deflection process. The regimes of the tire deflection process can be divided into two parts by the occurrence of tire bottoming. For a regime before tire bottoming, $m = 480{,}000$ and $r = 1.365$ (Ref. 16). For a regime after tire bottoming, the values of m and r become large numbers because a severe impact takes place when tire bottoming occurs.

On the other hand, the ER/MR shock struts are inflated to some finite pressure in the fully extended position. Thus, the shock strut does not begin to move under impact until sufficient force is developed to overcome the initial preloading imposed by the gas force.[15,16,18] Because the shock strut is effectively rigid in compression as well as in bending, the landing gear system may be considered to have only one degree of freedom during the initial stage of the impact. The equations of motion for the one-degree-of-freedom system are derived to permit determination of the initial conditions required for the analysis of the landing gear behavior subsequent to the beginning of shock strut motion.

Because $\ddot{z}_1 = \ddot{z}_2 = \ddot{z}$ and $\dot{z}_1 = \dot{z}_2 = \dot{z}$ during this first phase of the impact when the vertical force at the wheel axle F_{dv} is less than the initial gas force of the shock strut, $F_{g0}(= A_r P_{g0})$, so that $F_{dv} \leq |F_{g0}|$, the equation of motion can be given by

$$[(W_1 + W_2)/g]\ddot{z} + F_{ds} + F_t + L_f - W_1 - W_2 = 0 \tag{10}$$

where,

$$F_{dv} = F_t + (W_2/g)\ddot{z} - W_2 \tag{11}$$

Note that the states of Eq. (10) are used as initial conditions for solving Eq. (5). In addition, note that the yield force does not come into the condition of $F_{dv} \leq |F_{g0}|$ because there is no field input applied to the ER/MR shock strut at the initial impact.

To attenuate the dynamic load and vibration of the landing gear system, a robust sliding mode control algorithm is adopted in this study. It is well known that the robust sliding mode controller has strong stability characteristics in the presence of parameter variations and external disturbances.[19–21] The dynamics for the ER/MR landing gear system can be rewritten in the form of a single input nonlinear system

$$\ddot{z}_1 = (g/W_1)(-F_v - F_g - F_s + W_1 - u - L_f)$$

$$\ddot{z}_2 = (g/W_2)(F_v + F_g + F_s - F_t + W_2 + u) \tag{12}$$

where u is the control input that physically means the yield force F_y. To emulate the practical situation of control action, the dynamics for the yield force are modeled as[20]

$$\dot{F}_y^* = 100\left(u - F_y^*\right) \tag{13}$$

This model neglects higher-order dynamics from command control input u to actual yield force F_y^*. Note that Eq. (13) is used not for

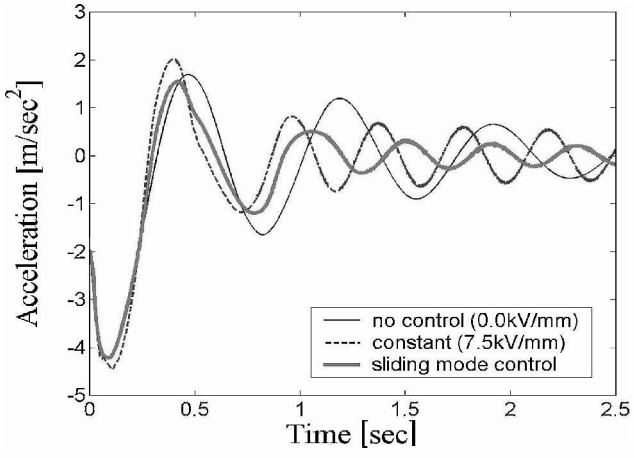

Acceleration of the upper mass

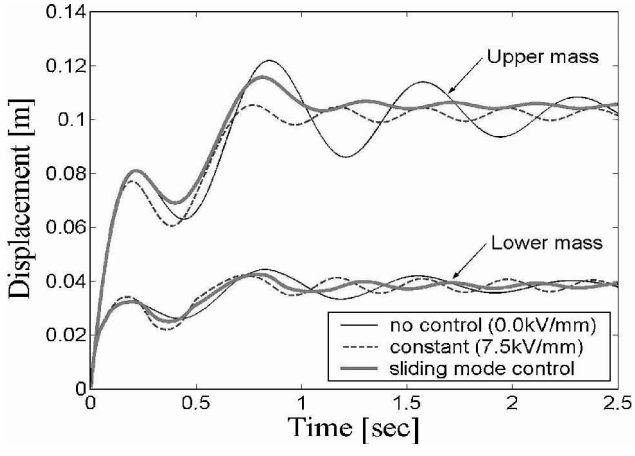

Displacement

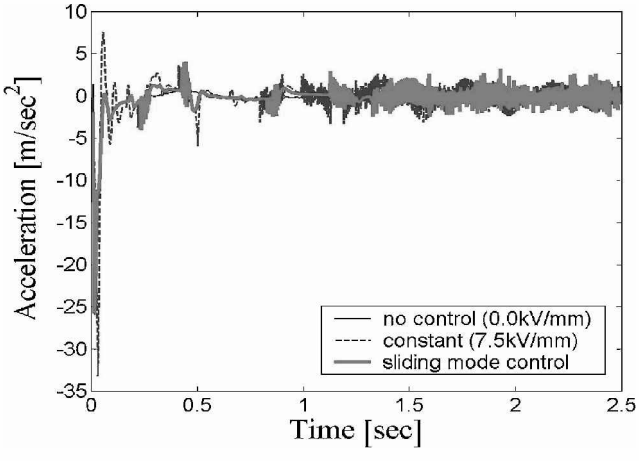

Acceleration of the lower mass

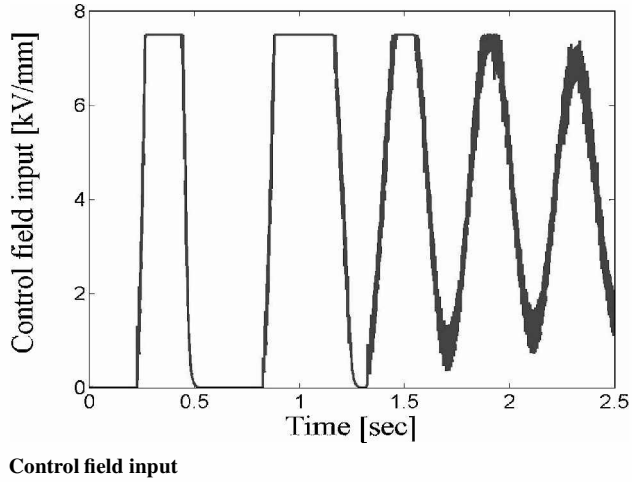

Control field input

Fig. 8 Controlled performance of the ER/MR landing gear system in case of carrying payload (sink velocity = 0.76 m/s).

the design of the controller, but for the performance evaluation of the simulated system.

Then, a sliding surface function is defined as follows

$$\psi = \left(\frac{\mathrm{d}}{\mathrm{d}t} + \lambda\right) z_1 \tag{14}$$

where $\lambda > 0$ is the slope of the sliding surface. For the practical ER/MR landing gear system, there are some variations in the parameters such as upper vehicle mass, viscous damping, and so forth. Therefore, in this study, the following parameter variations are considered in the design of the robust sliding mode controller:

$$500 \le W_1/g \le 800\text{kg} \tag{15}$$

$$1500 \le c(\dot{v}, G) \le 7000\,\text{N} \cdot \text{s/m} \tag{16}$$

$$70{,}000 \le k_s \le 90{,}000 \tag{17}$$

$$0 \le L_f \le 2(W_1 + W_2) \tag{18}$$

It is assumed that the estimation errors of the parameter variations and dynamics are bounded as follows

$$\bar{W}_1 \ge |W_1 - \hat{W}_1| \tag{19}$$

$$\bar{c}(\dot{v}, G) \ge |\hat{c}(\dot{v}, G) - c(\dot{v}, G)| \tag{20}$$

$$\bar{k}_s \ge |\hat{k}_s - k_s| \tag{21}$$

$$\bar{F}_g \ge |\hat{F}_g - F_g| \tag{22}$$

where, $\hat{W}_1$, $\hat{c}(\dot{v}, G)$, $\hat{k}_s$, and $\hat{F}_g$ are the estimates and $\bar{W}_1$, $\bar{c}(\dot{v}, G)$, $\bar{k}_s$, and $\bar{F}_g$ are the bounds on the estimation errors. Then we can formulate the robust sliding mode controller satisfying the sliding mode condition $\psi\dot{\psi} < 0$:

$$u = (\hat{W}_1/g)\lambda\dot{z}_1 - \hat{F}_v - \hat{F}_g - \hat{F}_s + \hat{W}_1 + k_g\,\text{sgn}(\psi) \tag{23}$$

where $\hat{F}_v$, $\hat{F}_g$, and $\hat{F}_s$ are the estimation dynamics for viscous damping force, gas spring force, and coil spring force; k_g is the discontinuous control gain given by

$$k_g = \bar{c}(\dot{v}, G)|\dot{z}_1 - \dot{z}_2| + \bar{F}_g + \bar{k}_s|z_1 - z_2| + \bar{W}_1 + \xi_v + (W_{1\max}/g)(1 + \phi_w)\lambda|\dot{z}_1| \tag{24}$$

where

$$\phi_w = W_{1\max}/W_{1\min}, \qquad \xi_v \ge 2(W_{1\max} + W_2) \tag{25}$$

Then, we can show that the controller u given by Eq. (23) satisfies the sliding mode condition, as follows:

$$\begin{aligned}\psi\dot{\psi} &= \psi[(g/W_1)(-F_v - F_g - F_s + W_1 - u - L_f) + \lambda\dot{z}_1] \\ &= \psi\{(g/W_1)[(\hat{F}_v - F_v) - \bar{c}(\dot{v}, G)|\dot{z}_1 - \dot{z}_2|\,\text{sgn}(\psi) \\ &\quad + (\hat{F}_g - F_g) - \bar{F}_g\,\text{sgn}(\psi) + (\hat{F}_s - F_s) - \bar{k}_s|z_1 - z_2|\,\text{sgn}(\psi) \\ &\quad + (W_1 - \hat{W}_1) - \bar{W}_1\,\text{sgn}(\psi) - L_f - \xi_v\,\text{sgn}(\psi)] \\ &\quad + (1 - \hat{W}_1/W_1)\lambda\dot{z}_1 - (W_{1\max}/W_1)(1 + \phi_w)\lambda|\dot{z}_1|\,\text{sgn}(\psi)\} < 0\end{aligned} \tag{26}$$

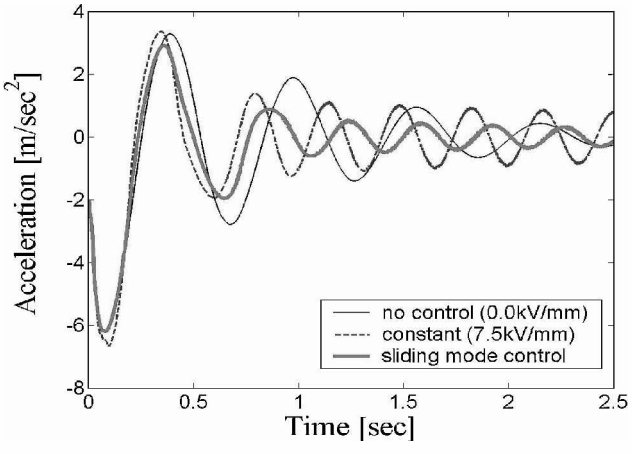

Acceleration of the upper mass

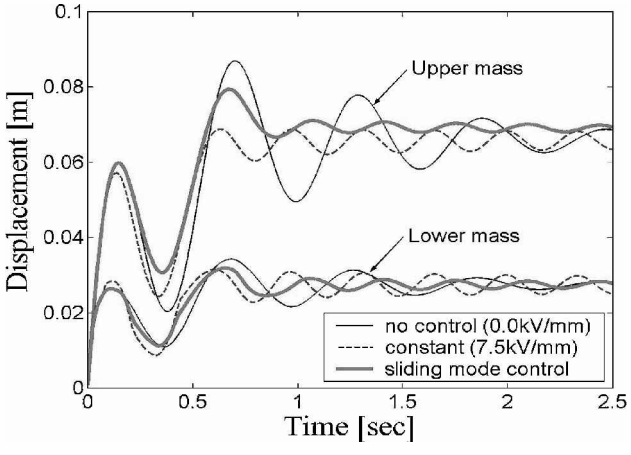

Displacement

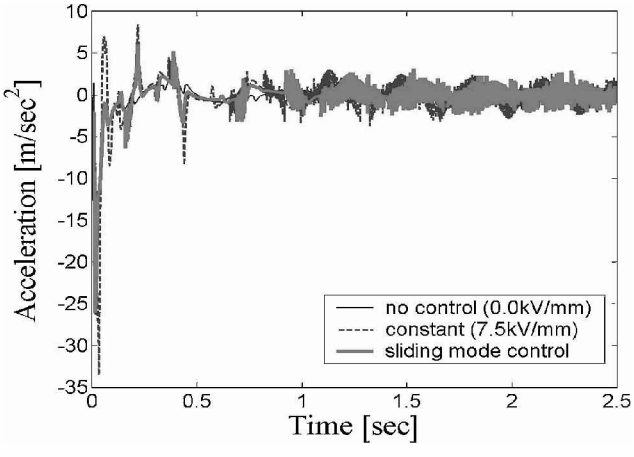

Acceleration of the lower mass

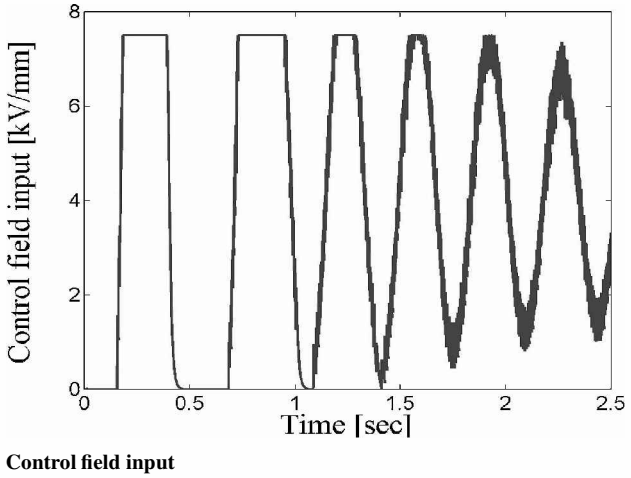

Control field input

Fig. 9 Controlled performance of the ER/MR landing gear system in case of zero payload (sink velocity = 0.76 m/s).

To attenuate the chattering in the control input, the sign function given by Eq. (23) is replaced by saturation function with an appropriate boundary thickness ε as follows:

$$u = (\hat{W}_1/g)\lambda\,\dot{z}_1 - \hat{c}(\dot{v}, G)(\dot{z}_1 - \dot{z}_2) - \hat{F}_g - \hat{k}_s(z_1 - z_2) + \hat{W}_1 + k_g\,\mathrm{sat}(\psi) \tag{27}$$

where

$$\mathrm{sat}(\psi) = \begin{cases} \psi/\varepsilon & \text{at} \quad |\psi| \le \varepsilon \\ \mathrm{sgn}(\psi) & \text{at} \quad |\psi| > \varepsilon \end{cases} \tag{28}$$

On the other hand, the proposed robust sliding mode control input is designed in the active actuator manner. However, because the ER/MR shock strut is a semi-active actuator, the following semi-active condition should be superposed on Eq. (27) (Refs. 21 and 22):

$$u = \begin{cases} u & \text{if} \quad u \cdot (\dot{z}_1 - \dot{z}_2) \ge 0 \\ 0 & \text{if} \quad u \cdot (\dot{z}_1 - \dot{z}_2) < 0 \end{cases} \tag{29}$$

This semi-active condition constrains the control input to ensure that the ER/MR landing gear system is dissipating energy.

Figure 8 presents controlled performance of the ER/MR landing gear system under the robust sliding mode controller. In this case, the upper mass is chosen as 800 kg, and the sink velocity of the aircraft is set to 0.76 m/s. It considers the practical condition that the aircraft carrying payload is landing softly. The system and control parameters employed in this study are specified in Table 1. As observed in Fig. 8, the accelerations of the upper and lower masses are significantly reduced by employing the robust sliding mode controller to the ER/MR landing gear system. In addition, the robust sliding mode controller gives good performance in displacement attenuation. On the other hand, it is observed that the control field input is discontinuous because of the semi-active constraint given by Eq. (29). In this study, the control field input is limited to 7.5 kV/mm.

Figure 9 shows controlled performance of the ER/MR landing gear system in case of zero payload. In this case, the upper mass is 500 kg. As observed, the acceleration of the upper mass is significantly increased because the aircraft mass is lighter than that of

Table 1 System and control parameters

Quantity	Symbol	Value	Units
Piston head area	A_p	2.0e−3	m^2
Piston rod area	A_r	1.96e−4	m^2
Initial gas pressure of pneumatic chamber	P_{g0}	1.1	MPa
Initial volume of pneumatic chamber	V_{g0}	4.36e−5	m^3
Stiffness coefficient of coil spring	k_s	80,000	N/m
Weight of lower mass	W_2	15.3	kg
Estimation error bound for viscous damping coefficient	$\bar{c}(\dot{v}, G)$	5,500	N · s/m
Estimation error bound for stiffness coefficient of coil spring	$\bar{k}_s$	20,000	N/m
Estimation error bound for upper mass	$\bar{W}_1$	300	kg
Estimation error bound for gas spring force	$\bar{F}_g$	$0.5\lvert F_g\rvert$	N
Estimate for viscous damping coefficient	$\hat{c}(\dot{v}, G)$	4,500	N · s/m
Estimate for stiffness coefficient of coil spring	$\hat{k}_s$	70,000	N/m
Estimate for weight of upper mass	$\hat{W}_1$	650	kg
Estimate for gas spring force	$\hat{F}_g$	$1.5F_g$	N
Bound for external disturbances	ξ_v	16,000	N
Slope of sliding surface	λ	10	——
Boundary thickness	ε	0.003	——

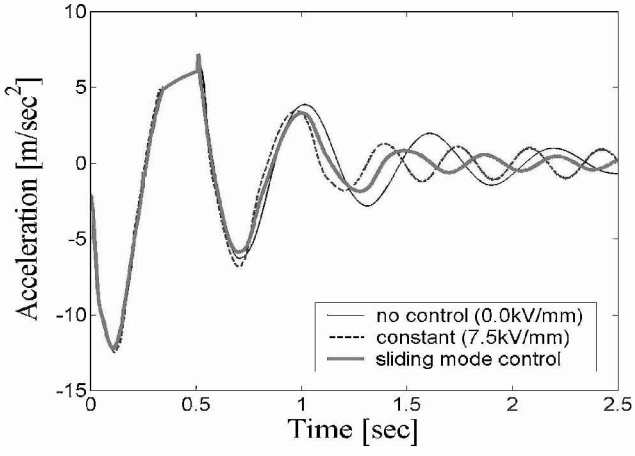

Acceleration of the upper mass

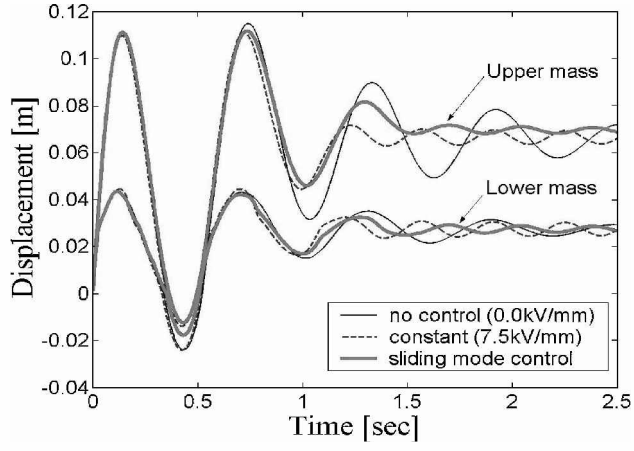

Displacement

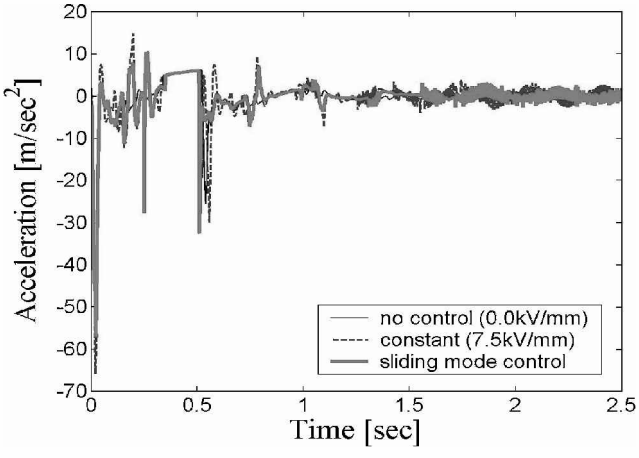

Acceleration of the lower mass

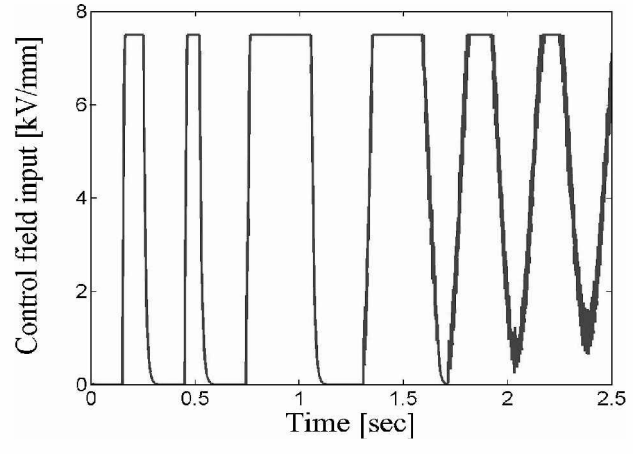

Control field input

Fig. 10 Controlled performance of the ER/MR landing gear system in case of zero payload (sink velocity = 1.37 m/s).

Fig. 8. However, the absolute displacement of the upper and lower masses is decreased, although its vibration is increased. Still, it is observed that the robust sliding mode controller gives good performance on attenuating the acceleration and displacement of the landing gear system. On the other hand, the case of zero payload requires a little more control field input to attenuate the vibration of the landing gear system. It arises from the vibration of the upper and lower masses in case of zero payload being greater than that of carrying payload case. When the sink velocity of the aircraft is increased to 1.37 m/s, controlled performance of the ER/MR landing gear system is as shown in Fig. 10. It considers that the aircraft with zero payload is landing normally. As observed, the sliding mode controller gives favorable vibration control performances.

Figure 11 presents comparison of the passive and ER/MR landing gear systems on vibration control performance at the sink velocity of 1.37 m/s. In this case, the passive landing gear system has the passive shock strut with 70% of critical viscous damping coefficient of the system, which is given by

$$c = 2 \times 0.7\sqrt{\left(k_s + nA_r^2 P_{g0}/V_{g0}\right)(W_1/g)} \tag{30}$$

In Fig. 11, the thin solid line stands for the passive landing gear system, the dashed line is for the ER/MR landing gear system with the length of $1 \times L$, and the thick solid line is for the ER/MR landing gear system with the length of $2 \times L$. As observed in Fig. 11a, both ER/MR landing gear systems show better suppression at the first and second peaks of the acceleration of the upper mass than

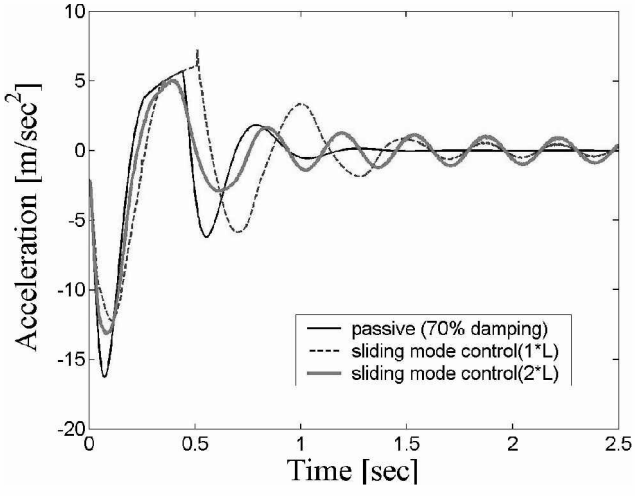

a) Acceleration of the upper mass

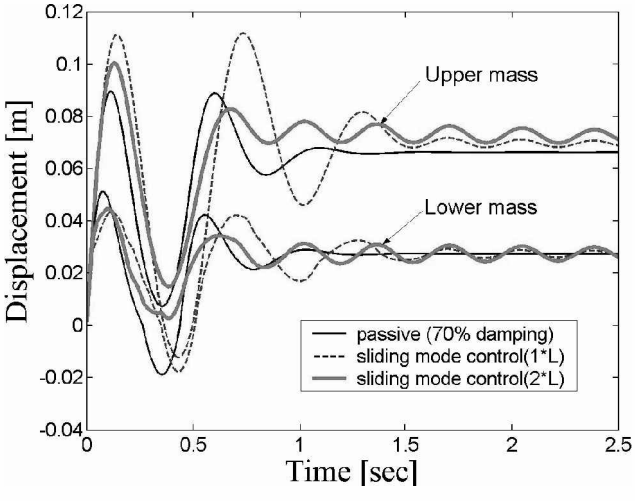

b) Displacement

Fig. 11 Comparison of the passive and ER/MR landing gear system in case of zero payload (sink velocity = 1.37 m/s).

the passive system. However, in the residual vibration of the upper mass, the passive landing gear system shows better controlled performance. Note that the peak acceleration reduction is a prior required function of the landing gear system. On the other hand, when the length is increased, the acceleration reduction at the first peak is deteriorated, but the control performance at the second peak is greatly improved. Figure 11b shows the displacement of the landing gear systems. As observed in Fig. 11b, the ER/MR landing gear system with the length of $1 \times L$ shows the relatively large vibration of the displacement as opposed to the passive system. However the ER/MR landing gear system with length of $2 \times L$ provides favorable control performance in the vibration reduction of the displacement, as well as the acceleration, when being compared with the passive system.

Conclusions

An analysis of a telescopic type of helicopter tail landing gear system using ER/MR shock struts was constructed, and its feasibility and effectiveness on attenuating the dynamic load and vibration were demonstrated. A theoretical model for ER/MR shock struts was developed based on experimental data obtained at different excitation velocities and fields for an ER shock strut constructed at the University of Maryland. With the theoretical model, the ER/MR landing gear system was constructed, and its governing equation was derived. From the obtained governing equation, a sliding mode controller, robust against parameter variations and external disturbances, was formulated to attenuate the acceleration and displacement of the landing gear system. It has been demonstrated that acceleration and displacement are significantly attenuated by employing the robust sliding mode controller to the ER/MR landing gear system, regardless of parameter variations such as upper vehicle mass, viscous damping, and so forth.

In the future, theoretical models incorporating practical effects such as hysteresis will be used to design the controller of the ER/MR landing gear system, and its implementation will be experimentally and theoretically evaluated. In addition, the controlled performance of the ER/MR landing gear system will be compared with existing landing gear systems through experimental and theoretical studies.

Acknowledgments

The authors acknowledge research support under the National Rotorcraft Technology Center's Rotorcraft Center of Excellence Program (Yung Yu as Technical Monitor). Instrumentation support was provided under the Defense University Research Instrumentation Program of the U.S. Army Research Office (Gary Anderson as Technical Monitor).

References

[1]Lee, H. G., Choi, S. B., Han, S. S., and Kim, J. H., "Bingham and Response Characteristics of ER Fluids in Shear and Flow Modes," *International Journal of Modern Physics B*, Vol. 15, Nos. 6 and 7, 2001, pp. 1017–1024.

[2]Carlson, J. D., Catanzarite, D. N., and St. Clair, K. A., "Commercial Magneto-Rheological Fluid Devices," *Proceedings of 5th International Conferences on ER Fluids, MR Suspensions and Associated Technology*, World Scientific, Singapore, Republic of Singapore, 1996, pp. 20–28.

[3]Lou, Z, Ervin, R. D., Filisko, F. E., and Winkler, C. B., "An Electrorheologically Controlled Semi-Active Landing Gear," Society of Automotive Engineers, SAE TP Series 931403, 1993.

[4]Choi, S. B., Choi, Y. T., Chang, E. G., Han, S. J., and Kim, C. S., "Control Characteristics of a Continuously Variable ER Damper," *Mechatronics*, Vol. 8, No. 2, 1998, pp. 143–161.

[5]Gavin, H. P., Hanson, R. D., and Filisko, F. E., "Electrorheological Dampers, Part I: Analysis and Design," *Journal of Applied Mechanics*, Vol. 63, No. 3, 1996, pp. 669–675.

[6]Gavin, H. P., Hanson, R. D., and Filisko, F. E., "Electrorheological Dampers, Part II: Testing and Modeling," *Journal of Applied Mechanics*, Vol. 63, No. 3, 1996, pp. 676–682.

[7]Gordaninejad, F., and Kelso, S. P., "Fail-Safe Magneto-Rheological Fluid Dampers for Off-Highway, High-Payload Vehicles," *Journal of Intelligent Material Systems and Structures*, Vol. 11, No. 5, 2001, pp. 395–406.

[8]Kamath, G. M., and Wereley, N. M., "Nonlinear Viscoelastic-Plastic Mechanism-Based Model of an Electrorheological Damper," *Journal of Guidance, Control, and Dynamics*, Vol. 20, No. 6, 1997, pp. 1125–1132.

[9]Lindler, J. E., and Wereley, N. M., "Analysis and Testing of Electrorheological Bypass Dampers," *Journal of Intelligent Material Systems and Structures*, Vol. 10, No. 5, 1999, pp. 363–376.

[10]Lindler, J. E., and Wereley, N. M., "Double Adjustable Shock Absorbers Using Electrorheological Fluid," *Journal of Intelligent Material Systems and Structures*, Vol. 10, No. 8, 1999, pp. 652–657.

[11]Kamath, G. M., Wereley, N. M., and Jolly, M. R., "Analysis and Testing of a Model-Scale Magnetorheological Fluid Helicopter Lag Mode Damper," *Journal of American Helicopter Society*, Vol. 44, No. 3, 1996, pp. 234–248.

[12]Wereley, N. M., Kamath, G. M., and Madhavan, V., "Hysteresis Modeling of Semi-Active Magnetorheological Helicopter Dampers," *Journal of Intelligent Material Systems and Structures*, Vol. 10, No. 8, 1999, pp. 624–633.

[13]Kim, K., and Jeon, D., "Vibration Suppression in an MR Fluid Damper Suspension System," *Journal of Intelligent Material Systems and Structures*, Vol. 10, No. 10, 1999, pp. 779–786.

[14]Sims, N. D., Peel, D. J., Stanway, R., Johnson, A. R., and Bullough, W. A., "The Electrorheological Long-Stroke Damper: A New Modelling Technique with Experimental Validation," *Journal of Sound and Vibration*, Vol. 229, No. 2, 2000, pp. 207–227.

[15]Milwitzky, B., and Cook, F. E., "Analysis of Landing Gear Behavior," NACA Rept. 1154, 1953.

[16]Reddy, P. J., Nagaraj, V. T., and Ramamurti, V., "Analysis of a Semi-Levered Suspension Landing Gear with Some Parametric Study," *Journal of Dynamic Systems, Measurement and Control*, Vol. 218, No. 3, 1984, pp. 218–224.

[17]Wahi, M. K., "Oleopneumatic Shock Strut Dynamic Analysis and Its Real-Time Simulation," *Journal of Aircraft*, Vol. 13, No. 4, 1976, pp. 303–308.

[18]Yadav, D., and Ramamoorthy, R. P., "Nonlinear Landing Gear Behavior at Touchdown," *Journal of Dynamic Systems, Measurement and Control*, Vol. 113, No. 4, 1991, pp. 677–683.

[19]Slotine, J. J., and Li, W., "Sliding Control," *Applied Nonlinear Control*, Prentice–Hall Upper Saddle River, NJ, 1991, pp. 276–310.

[20]Hedrick, J. K., and Gopalswamy, S., "Nonlinear Flight Control Design via Sliding Methods," *Journal of Guidance, Control, and Dynamics*, Vol. 13, No. 3, 1990, pp. 850–858.

[21]Choi, S. B., Choi, Y. T., and Park, D. W., "A Sliding Mode Control of a Full-Car Electrorheological Suspension System via Hardware-in-the-Loop Simulation," *Journal of Dynamic Systems, Measurement and Control*, Vol. 122, No. 1, 2000, pp. 114–121.

[22]Karnopp, D., Crosby, M. J., and Harwood, R. A., "Vibration Control Using Semi-Active Force Generators," *Journal of Engineering for Industry*, Vol. 96, No. 2, 1974, pp. 619–626.